



저작자표시-비영리-변경금지 2.0 대한민국

이용자는 아래의 조건을 따르는 경우에 한하여 자유롭게

- 이 저작물을 복제, 배포, 전송, 전시, 공연 및 방송할 수 있습니다.

다음과 같은 조건을 따라야 합니다:



저작자표시. 귀하는 원저작자를 표시하여야 합니다.



비영리. 귀하는 이 저작물을 영리 목적으로 이용할 수 없습니다.



변경금지. 귀하는 이 저작물을 개작, 변형 또는 가공할 수 없습니다.

- 귀하는, 이 저작물의 재이용이나 배포의 경우, 이 저작물에 적용된 이용허락조건을 명확하게 나타내어야 합니다.
- 저작권자로부터 별도의 허가를 받으면 이러한 조건들은 적용되지 않습니다.

저작권법에 따른 이용자의 권리는 위의 내용에 의하여 영향을 받지 않습니다.

이것은 [이용허락규약\(Legal Code\)](#)을 이해하기 쉽게 요약한 것입니다.

[Disclaimer](#)

Master's Thesis

Concrete Static Stress Estimation Using Computer  
Vision-Based Digital Image Processing

Eun Jin Kim

Department of Urban and Environmental Engineering  
(Urban Infrastructure Engineering)

Graduate School of UNIST

2018

# Concrete Static Stress Estimation Using Computer Vision-Based Digital Image Processing

Eun Jin Kim

Department of Urban and Environmental Engineering  
(Urban Infrastructure Engineering)

Graduate School of UNIST

# Concrete Static Stress Estimation Using Computer Vision-Based Digital Image Processing

A thesis

submitted to the Graduate School of UNIST

in partial fulfillment of the

requirements for the degree of

Master of Science

Eun Jin Kim

07/04/2018

Approved by



---

Advisor

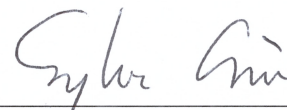
Sung-Han Sim

# Concrete Static Stress Estimation Using Computer Vision-Based Digital Image Processing

Eun Jin Kim

This certifies that the thesis/dissertation of Eun Jin Kim is approved.

07/04/2018




Advisor: Sung-Han Sim

Associate Professor  
School of Urban and Environmental Engineering  
Ulsan National Institute of Science and Technology (UNIST)



Myoungsu Shin: Thesis Committee Member #1

Associate Professor  
School of Urban and Environmental Engineering  
Ulsan National Institute of Science and Technology (UNIST)



Young Joo Lee: Thesis Committee Member #2

Assistant Professor  
School of Urban and Environmental Engineering  
Ulsan National Institute of Science and Technology (UNIST)

## Abstract

As increasing interests about structural safety due to occasionally occurring collapse of structures and social infrastructures, efforts to identify and monitor the current state of structure are also increasing. Recently, most structures have been built of concrete, so identification of safety level of concrete structures becomes a critical issue. One of such techniques is to evaluate the current stress state in concrete. This technique is essential in various fields involved in an investigation of tensile stress of tendons in pre- and post-tensioned structures, building remodeling which needs to remove bearing walls and adds other foundations, and identification of load distribution in enlarged concrete structures. In other words, current stress level in concrete is an important factor to check the safety level of the structures in service.

Although it is obvious that a technique for estimating the static stress level of concrete is essential, the method to identify the stress state of the currently used concrete structure is definitely limited. Several efforts for estimating the current stress state have been developed in previous research, including a stress-strain relationship based on elastic theory and a stress relaxation method (SRM) for concrete. These methods in the previous researches have made a certain contribution in this field but practical use in real structures is still inadequate. Therefore, an objective of this study is to develop a static stress estimation technique which can be applied to real concrete structures. This study proposes a method that can measure the static stress level of concrete by incorporating SRM and computer vision-based image processing. Applying a small damage to concrete specimen can release the current stress state and induce stress field change inside concrete around the damage. Computer vision-based measurement can measure the deformation due to this stress field change. This deformation measurement is used in the static stress estimation algorithm developed in this study. The proposed method is validated using several concrete specimens and consequently demonstrates the performance.



## Contents

ABSTRACT.....	.....
CONTENTS.....	I
LIST OF FIGURES .....	II
LIST OF TABLES.....	III
CHAPTER 1. INTRODUCTION.....	1
CHAPTER 2. RESEARCH BACKGROUND .....	3
2.1 Previous research for concrete stress estimation.....	3
2.2 Stress Relaxation Method .....	4
2.3 Digital image correlation .....	8
CHAPTER 3. CONCRETE STATIC STRESS ESTIMATION.....	10
CHAPTER 4. PARAMETRIC ANALYSIS: Effect of hole diameter and depth .....	17
CHAPTER 5. EXPERIMENTAL VALIDATION.....	20
5.1 Experimental setup.....	20
5.2 Results and analysis .....	23
CHAPTER 6. CONCLUSION.....	28
REFERENCES .....	30



## List of Figures

Figure 1 Experimental configuration for partial sectioning method.....	4
Figure 2 Comparison between hole-drilling and core-drilling.....	5
Figure 3 Rosette strain gauges for residual stress measurements in hole-drilling method .....	5
Figure 4 Experimental figures of the previous research .....	6
Figure 5 Digital Image Correlation (DIC) .....	8
Figure 6 Graphical user interface of ‘Ncorr’ .....	9
Figure 7 Examples of using ‘Ncorr’ .....	9
Figure 8 Overview of the proposed method.....	10
Figure 9 Main idea of static stress estimation algorithm .....	11
Figure 10 Flowchart of the static stress estimation algorithm .....	11
Figure 11 Displacement field data of experiment and FE model.....	12
Figure 12 Matched both planes and normal vectors through coordinate transform.....	14
Figure 13 Final transformed displacement field shape of experimental and FE analysis data .....	16
Figure 14 FE modelling in Parametric analysis .....	17
Figure 15 Mean displacement along change of parameters .....	18
Figure 16 Compressive strength test on the concrete specimen .....	20
Figure 17 Stress-strain curve of concrete specimen.....	21
Figure 18 Concrete specimen dimension.....	22
Figure 19 Experimental configuration .....	23
Figure 20 Pictures before and after hole-drilling and DIC results – Type 1_Test3 .....	24
Figure 21 Experimental results – Type 1_Test3 .....	25
Figure 22 Pictures before and after hole-drilling and DIC results – Type 2_Test10.....	25
Figure 23 Experimental results – Type 2_Test10.....	26
Figure 24 Experimental results .....	27

## List of Tables

Table 1 Comparison between previous SRM researches for concrete .....	7
Table 2 FE modelling condition .....	12
Table 3 FE modelling condition in parametric analysis.....	17
Table 4 Compressive strength test of concrete specimen .....	21
Table 5 Experimental condition.....	23
Table 6 Experimental results .....	27



## CHAPTER 1. INTRODUCTION

Concrete is the most commonly used construction material in the world. A wide variety of current structures are constructed with concrete since it has a number of advantages; low price, casting to any desired shape, high compressive strength and durability. As tremendous people use these structures, the issue to maintain and manage the structures is becoming more important for sustainable and safe society. According to increasing interests about the safety of concrete structures due to preventing collapse of structures and social infrastructures, efforts to identify and monitor the current state of the structure are also increasing. Recently, most structures have been built with concrete, so identification of safety level of concrete structures becomes a critical issue.

One of the poor properties of concrete is that concrete is a brittle material, which is vulnerable to sudden failure. Thus, notification of the current concrete state in structures is essential to prevent unexpected collapse. One significant information in structures is to recognize the current stress level in concrete. The current stress state in concrete is an essential factor to check the deterioration and the current load distribution of structures in service. Technique to evaluate the stress condition in the concrete becomes a critical issue. Various fields require to develop this technique involved in tensile force measurement in a tendon of PSC bridges and architectural building remodeling [1-3]. However, once the structures have been built with concrete, identification of the stress level in concrete is challenging work. Despite its importance and usefulness, relatively little effort has been reported to developing the stress evaluation of concrete structures. In other words, identification of load distribution and current stress state inside concrete remains a challenging task even though this information is a significant issue to monitor safety of concrete structures.

In most cases, stress condition in concrete structures was investigated by calculating standardized formula [4]. However, the theoretical formula cannot satisfy various environmental and individual structural conditions, and this problem can induce to provide incorrect stress estimation results. To supplement the conventional method, several approaches to estimate current stress condition in concrete have been developed [5-11]. The commonly used method is using stress-strain relationship. Many researches had been conducted to establish the relationship between stress and strain of concrete [5-8] in various conditions. Saetta et al. [9] examined stress analysis considering thermal effects on the concrete based on stress-strain analysis. Fedele and Maier [10] conducted flat-jack tests and numerical simulation for the identification of stress states in concrete dam. Meanwhile, a stress relaxation method (SRM) for stress estimation is becoming widespread. SRM is a technique to measure a residual stress

in object by applying small damage. A variety of researchers chose this technique to estimate in-situ stress in concrete [12-20]. In their researches, deformation was measured with strain gauges or vision-based measurement technique and this information is converted to the in-situ stress estimation based on elastic theory. These researches have some limitations in being applied to real structures which may include uncertainties of the concrete, particularly elastic modulus, the limited number of measurement points and applying large size of damage that may cause the structural problem although they have made some contribution in this field.

In addition to SRM technique, digital image correlation (DIC) is selected as a vision-based digital image processing technique in previously mentioned research cases [14,16,18,19]. By making a small damage on the concrete surface, the current static stress level in concrete can be released and the corresponding released deformation near a damage can be recognized by a DIC technique. One of great advantages is that DIC can entirely measure the deformation at the user-desirable region. Using DIC, full-field deformation measurement can be performed, and it is subsequently used to estimate the current static stress in concrete.

This study presents that the static stress in the concrete can be estimated using both stress SRM technique and computer vision-based digital image processing while minimizing damage size. Static stress estimation algorithm has been developed to identify the optimal static stress in concrete. Parametric analysis is conducted to determine the hole size including diameter and depth. By using the algorithm and parametric analysis, the experimental errors can be calibrated which may include ununiform and inhomogeneous loading distribution and the abnormal state of the concrete specimen. The proposed method including the developed optimization algorithm is validated through laboratory-scale experiments on several concrete specimens and demonstrated its performance within 15 % error.

## CHAPTER 2. RESEARCH BACKGROUND

The objective of this study is to estimate static stress in concrete. In this chapter, some explanation of the research background which was used in this study is provided to help understanding. First, previous research for concrete stress estimation is summarized, then the stress relaxation method which is one of the commonly used methods for concrete stress estimation is followed. This study uses the stress relaxation method with computer vision-based deformation measurement technique, and digital image correlation technique is selected for vision-based measurement. So, a description of the digital image correlation is subsequently followed.

### 2.1 Previous research for concrete stress estimation

In recent years, a number of researchers have recognized the need for concrete stress estimation techniques and several approaches to estimate the current stress condition in concrete have been developed. First approach was the method using stress-strain relationship of concrete. Some researches had been conducted to establish the relationship between stress and strain of concrete and to investigate the concrete stress state based on strain measurement [5-8] in various conditions. Saetta et al. [9] examined stress analysis considering thermal effects on concrete dam and box-girder based on stress-strain analysis using a numerical method. However, the method using stress-strain relationship of concrete has some limitations. Since the initial stress state of concrete cannot be known, only the amount of stress change due to external load after strain gauge attachment can be known according to elastic theory. Other approach was the method using numerical simulation. Fedele and Maier [10] conducted flat-jack tests, numerical simulation and inverse analysis for the identification of stress states in concrete dam. In particular, Fedele et al. [11] proposed an experimental-numerical strategy for identification of in situ stresses in concrete dams using numerical validation and neural networks which was used in parameter identification.

Meanwhile, the stress relaxation method (SRM) is newly becoming widespread for stress estimation in concrete. In Korea, Park and Kim [4] suggested a practical method for estimating the concrete stress state in existing concrete structures using ‘partial sectioning method’ which is a kind of SRM techniques (see Figure 1). In their research, the effect of cutting interval ( $d$  in Fig. 1) and cutting

depth ( $h$  in Fig. 1) was considered and optimal values were found and used in partial sectioning method using FE analysis. The developed method was validated in actual existing concrete bridges and the results showed the feasibility with improving reliability comparing to theoretical calculations.

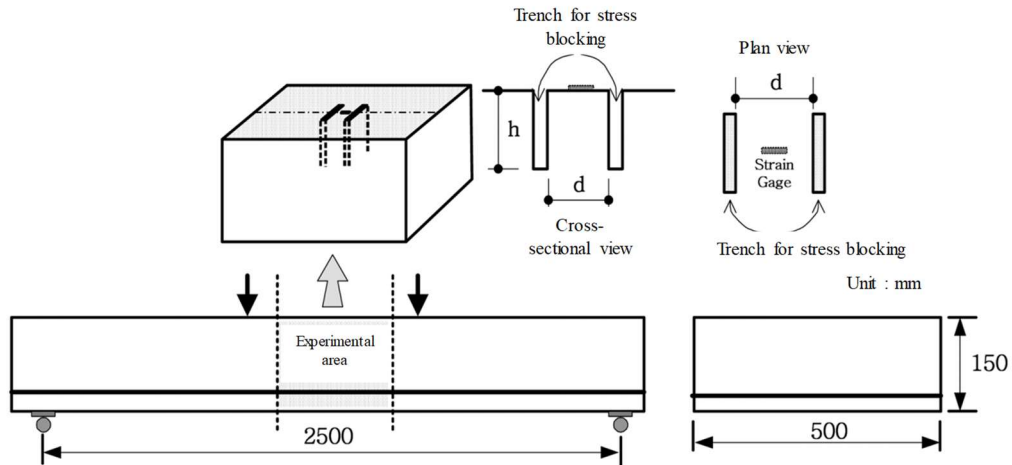


**Figure 1. Experimental configuration for partial sectioning method [4]**

## 2.2 Stress Relaxation Method (SRM)

A stress relaxation method (SRM) is a semi-destructive technique that assesses the current stress state by applying a small damage. The applied small damage in a stressed object can make the change of initial stress condition and lead to small deformation near the damage. SRM is a method to measure this deformation and estimate the residual stress. The SRM was first developed in the 1930s [21] and among several SRM technique, the most widely used methods are hold-drilling method and core-drilling method (or often called ring-core method) [22] as illustrated in Fig. 2 and rosettes strain gauges for residual stress measurement which was in hole-drilling method [23] are illustrated in Fig. 3. Hole-drilling method is an effective way to evaluate a residual stress condition with relatively less destructive and low cost. This method had been prescribed and updated in the ASTM standard by many researchers [24-26]. Core-drilling method needs a relatively larger diameter core than that of the hole-drilling method. This method is less affected to various error factors such as measurement and cutting tools. A number of researches using SRM have been implemented in various fields [27-31] and SRM have been demonstrated to be an effective technique for estimating the residual stresses in the object.

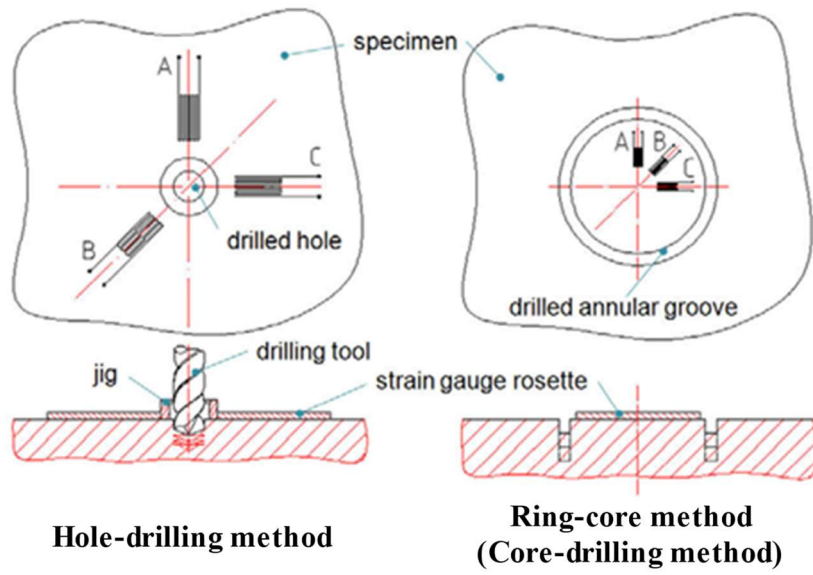


Figure 2. Comparison between hole-drilling and core-drilling [22]

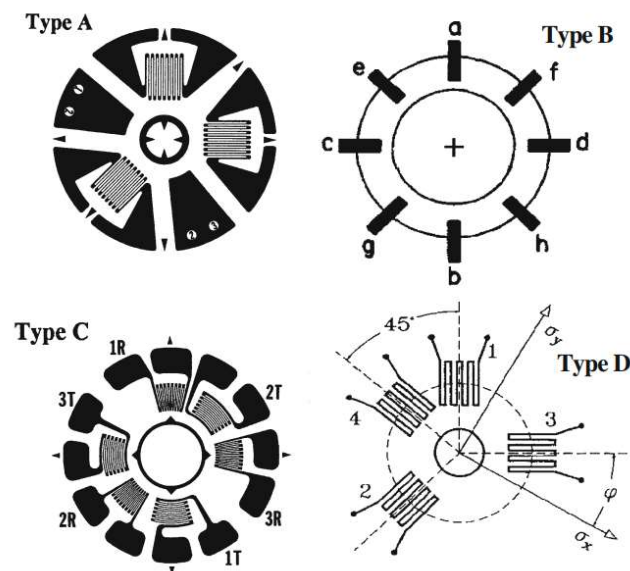


Figure 3. Rosette strain gauges for residual stress measurements in hole-drilling method [23]



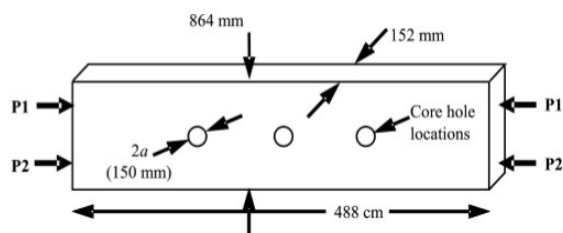
Efforts to apply the SRM to concrete have been conducted (see Fig. 4). Owens [12] firstly introduced the SRM using strain gauges to estimate the in-situ stress in concrete. Since concrete is a heterogeneous material and it can cause unintended and random responses during SRM, core-drilling method had been generally preferred in concrete for SRM [13-20] rather than hole-drilling method. Parivallas et al. [17] used vibrating wire strain gauges to measure released strain and suggested calibration coefficient to estimate in-situ stress of concrete. Trautner et al. [18] and McGinnis and Pessiki [19] measured static stress condition with a 10% error on pre-stressed concrete beams using core-drilling method. Ruan and Zhang [20] worked on in-situ stress identification using core-drilling and influence function and estimated stress about 10% error on the concrete specimen. Table 1 shows the summary of the previous SRM researches.



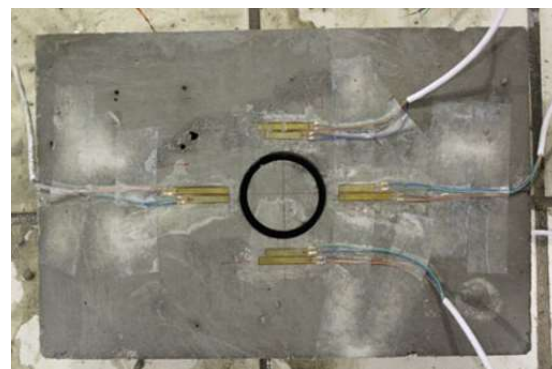
(a) Parivallas et al. (2011) [17]



(b) Trautner et al. (2011) [18]



(c) McGinnis and Pessiki (2015) [19]



(d) Ruan and Zhang (2015) [20]

**Figure 4. Experimental figures of the previous research**

**Table 1. Comparison between previous SRM researches for concrete**

	SRM technique	Measurement sensor	Damage size (mm)		Error (%)
			Diameter	Depth	
Owens (1993) [12]	Hole-drilling	Strain gauge	75	50 ~ 100	5.3
Parivallas et al. (2011) [17]	Core-drilling	Strain gauge	50	30	-
Trautner et al. (2011) [18]	Core-drilling	Digital image correlation	150	15 ~ 311	10
McGinnis and Pessiki (2015) [19]	Core-drilling	Digital image correlation	150	152	10
Ruan and Zhang (2015) [20]	Ring core-drilling	Strain gauge	53	50	< 10

These efforts contain several limitations to investigate the accurate stress condition in concrete structures. First important limitation is a size of the core. The size of the core was generally large compared with that of hole and the outer diameter of the core in previous researches was from 50 mm to 150 mm [13-20]. This may include some difficulties to recover after the experiment or may cause structural defects in real structures. Another is measurement tools. Deformation due to SRM was commonly measured with strain gauges in most researches. In general, strain gauge was used to measure the released deformation and some relationship between measured values were explained to derive static stress in concrete [20-26]. However, a limited number of strain gauge is used in this method and it may cause less accuracy due to using the average value of the limited measurement points. In order to overcome these limitations, this study intends to introduce a method to measure the full-field around the applied damage using the vision-based image processing technique.

To summarize the limitation of previous SRM researches to be applied to concrete structures,

- Released deformation by SRM was captured by Rosette strain gauges.
- Large damage is needed to attach the strain gauges and measured the deformation.
- The number of strain gauges and measurement points is limited.
- It leads to less accurate results due to using limited measurements.

### 2.3 Digital image correlation (DIC)

Computer vision-based digital image processing approaches provide a convenient and effective means of measuring deformation. Digital image correlation (DIC) is one of the most widely used image processing methods. DIC is a non-contact deformation measurement technique using several images before and after deformation, and it can track the movement of each subset pixel by calculating the correlation which has the maximum value between 0 to 1 as shown in Fig. 5. To perform the DIC, small and irregular speckles need to be densely painted on the objective surface and this randomness can make a comfortable correlation calculation of pixels in DIC. DIC has been used in various fields ranging from microscopic deformation measurement to deformation measurement of large structure [26-36] and the efforts to apply DIC to concrete also have been conducted [37-39].

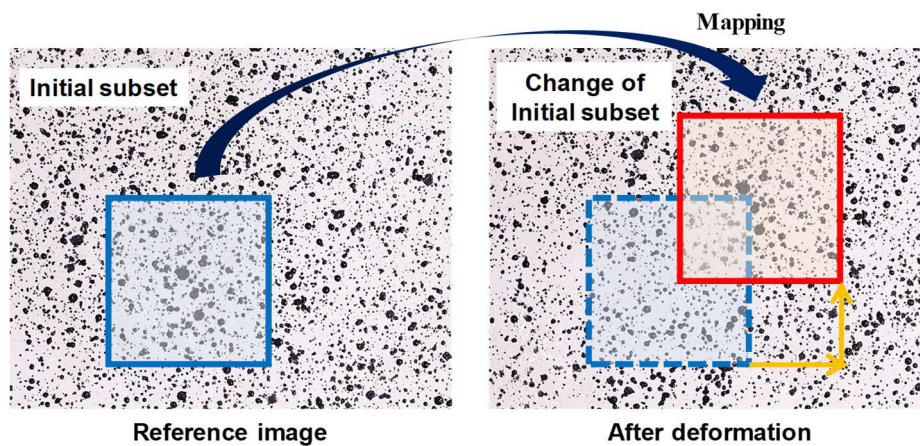


**Figure 5. Digital Image Correlation (DIC)**

DIC technique which can measure the desired full-field displacements had been introduced to overcome the limited measurement points in SRM. Some researches were performed with DIC to measure the deformation of concrete during SRM. Trautner et al. [18] worked identification of in-situ stresses in concrete using core-drilling method and DIC. In their work, the released displacements were measured by DIC instead of a strain gauge. Although the displacements were acquired on entire region around the core, the displacements which were not measured by DIC were linearly interpolated and three measurements were used to calculate the in-situ stress. Their work made a big contribution to evaluate the in-situ stress in concrete using both SRM and DIC with 10% error. However, it still remains

a problem of a big core size (150 mm diameter) and this may cause some troubles when applied to real structures.

In this paper, ‘Ncorr’ MATLAB software developed by the Georgia Institute of Technology [40-42] has been selected as a DIC software. ‘Ncorr’ is an open-source 2D DIC MATLAB software and it provides accessible and intuitive graphical user interface (GUI) as shown in Fig. 6. Examples of using ‘Ncorr’ are shown in Fig. 7. ‘Ncorr’ provides various types of measurement values such as strain and displacement. Since strain is obtained by the spatial differential of the displacement, it is quite vulnerable to the noise around the hole that can be generated in the drilling. To minimize the influence of that noise, the size of the hole should be increased. However, the objective of this study is to estimate the stress of the concrete with the minimum damage size. Therefore, displacement measurement is used in this study instead of using the strain which should follow the increasing hole size.

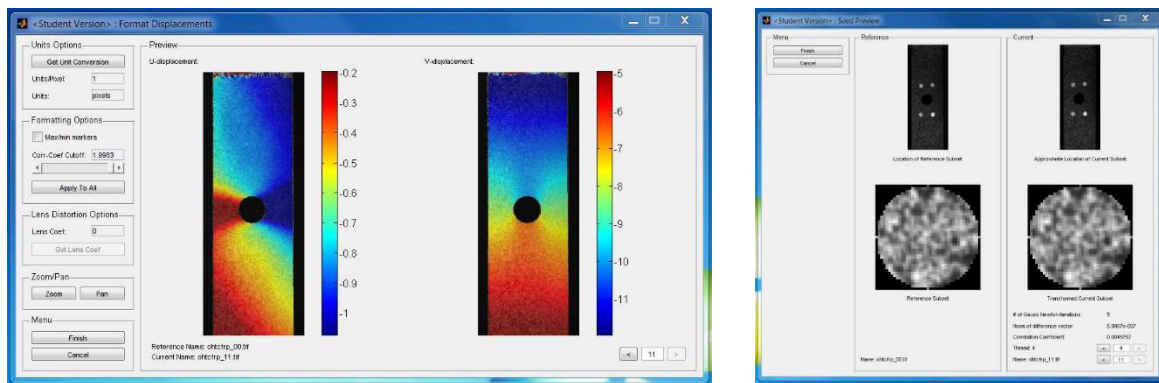


Figure 6. Graphical user interface of ‘Ncorr’ [40]

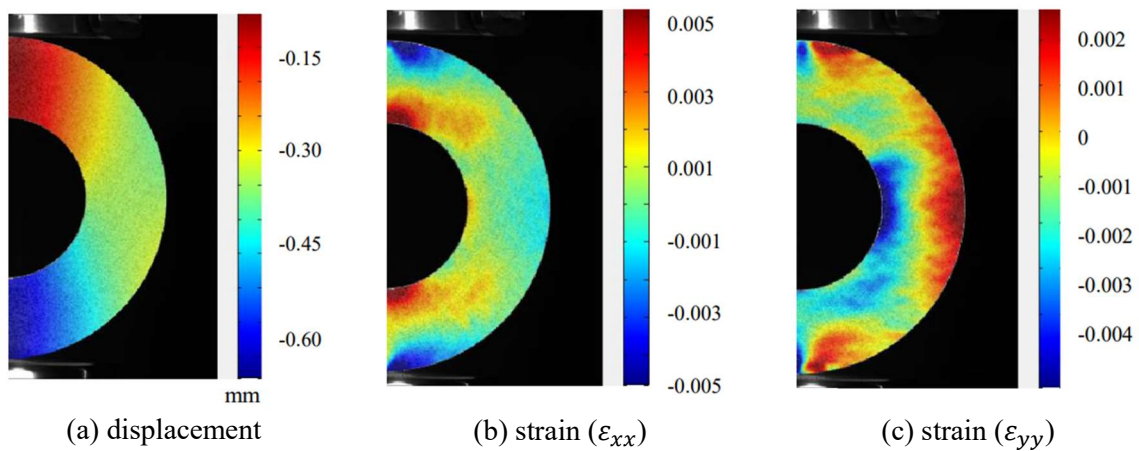
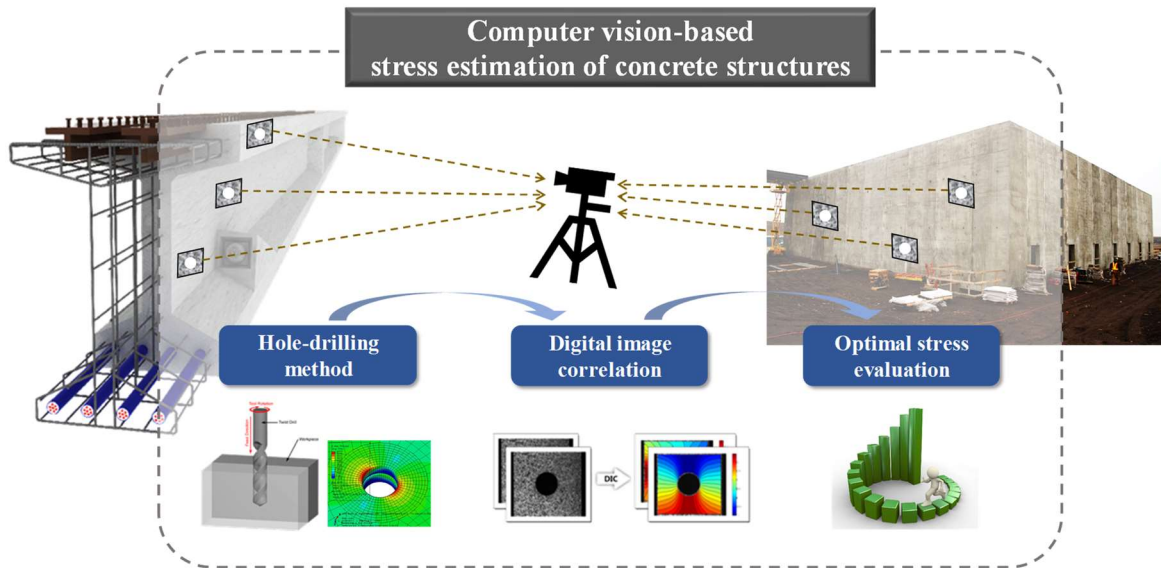


Figure 7. Examples of using ‘Ncorr’ [4140]

### CHAPTER 3. CONCRETE STATIC STRESS ESTIMATION

This study proposes the static stress estimation method for concrete which combines SRM, DIC and newly developed stress estimation algorithm. Overview figure of the proposed method is illustrated in Fig. 8. Hole-drilling method is selected as an SRM to reduce the damage size and the released deformation near hole is measured by DIC. Obtained experimental displacement data can be optimized to evaluate the static stress in concrete through optimization process.



**Figure 8. Overview of the proposed method**

In optimal stress evaluation step, the newly developed algorithm for stress estimation is involved, which requires both data sets of experimental and FE models. FE model data can be obtained using commercial software, ABAQUS. The main idea is to find the optimal stress such that displacement fields of experiment and FE model match well (see Fig. 9). Those figures in Fig. 9 represent the displacement field data around a hole at the experiment and FE analysis, respectively. As shown in Fig. 9, it seems that those two figures have similar shape, so the main idea of the proposed algorithm is to determine the optimal stress value which minimizes the difference of displacement field shape between experimental and FE model. It is assumed that displacement data in FE analysis depends on stress level

when it is under loading within elastic range. These two data will be used to estimate the static stress using the following a series of process. Flowchart of the proposed algorithm is illustrated in Fig. 10. It consists of two steps; Step 1: Coordinate transform of experimental displacement and Step 2: Optimal determination of the static stress.

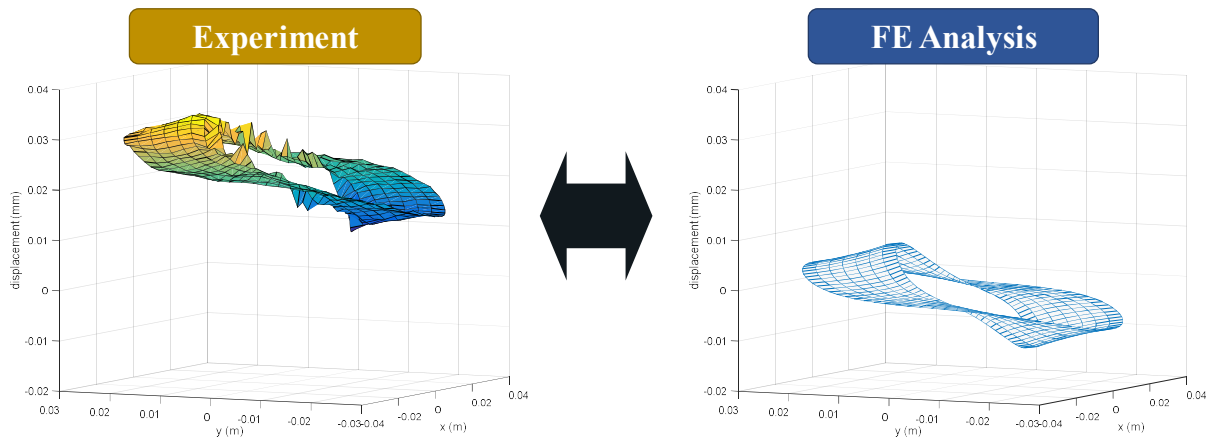


Figure 9. Main idea of static stress estimation algorithm

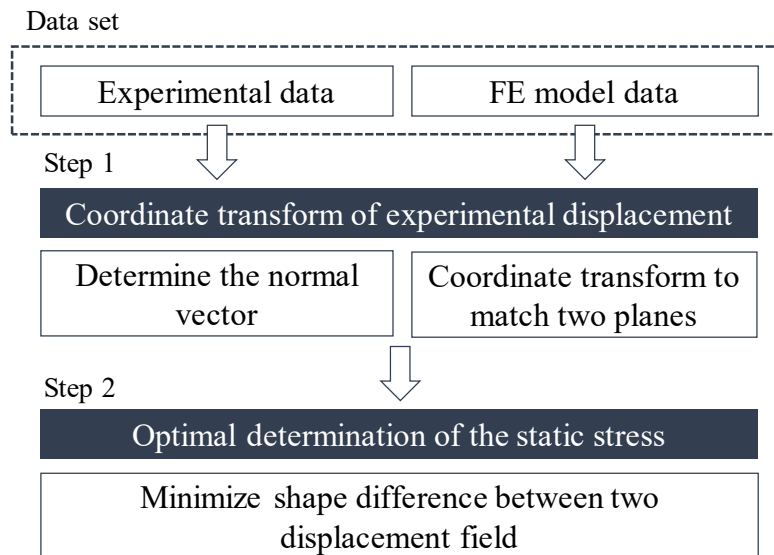


Figure 10. Flowchart of the static stress estimation algorithm

■ **STEP 1: Coordinate transform of experimental displacement**

In the first step, coordinate transform is conducted. The FE model of the concrete specimen is modeled as a reference using commercial software, ABAQUS. The FE model is designed to have the same properties with the actual concrete specimen and experimental condition which was used in real experiments. Detail description is represented in Table 2. Thus, released displacement field data around the hole due to hole-drilling can be obtained from experiment and FE analysis.

**Table 2. FE modelling condition**

Concrete specimen size	100mm×100mm×400mm
Elastic modulus	24.9GPa
Hole diameter	20mm
Hole depth	40mm
Loading stress	15MPa

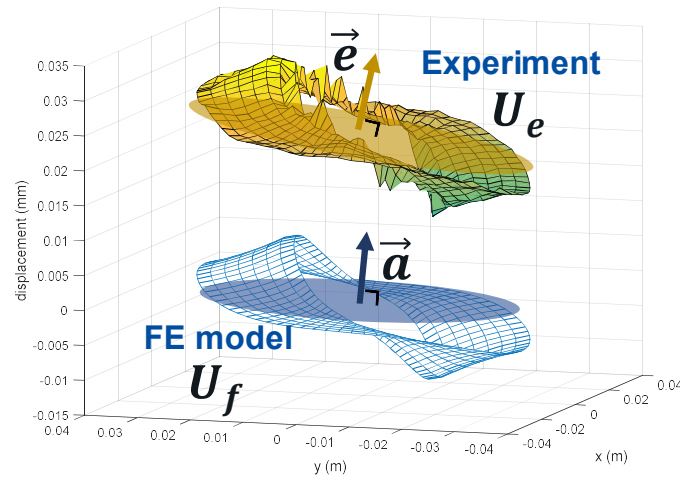


**Figure 11. Displacement field data of experiment and FE model**

Fig. 11 shows the plotted displacement field of each data. One noticeable thing in Fig. 11 is that a certain plane is penetrating each data set. In other words, each data set can be represented to the

particular plane and its normal vector which penetrates through data as shown in Fig. 11. Through this feature, a relationship between two data sets can be obtained by calculating the equation of the plane and its normal vector. To determine the normal vector of each plane which is made by displacement field as shown in this Fig. 11, the least square method is used. Then, the obtained normal vectors are used to coordinate transform to match two planes. In Fig. 11,  $\vec{e}$  and  $\vec{a}$  means normal vectors of experiment and FE analysis, respectively. Likewise,  $U_e$  and  $U_f$  means displacement field data of experiment and FE analysis, respectively.

Eq. (1) is the general equation of the plane, and its normal vector,  $\vec{n}$ , is denoted in Eq. (2) where  $a$ ,  $b$  and  $c$  are the components of normal vector. In Eq. (1),  $x$  and  $y$  values represent the location in the cylindrical coordinate system and  $z$  values are the obtained displacement values.  $d$  is the distance from the origin to the plane.

$$ax + by + cz = d \quad (1)$$

$$\vec{n} = \begin{bmatrix} a \\ b \\ c \end{bmatrix} \quad (2)$$

To solve the normal vector of each data, the least square method can be used, and general regression equation is shown in Eq. (3).  $A$  is a matrix composed of  $x$ ,  $y$ , and  $z$  in Eq. (1) and this matrix has a size of the number of data points by 3.  $B$  is a vector composed of  $d$  in Eq. (1). Final result,  $\vec{n}$ , in Eq. (4) shows the normal vector of each plane and it is used to identify the relationship between both data. Here,  $A^\dagger$  in Eq. (4) means pseudo inverse of matrix. After calculating normal vectors, angle,  $\theta$ , between them can be determined using Eq. (5).

$$A\vec{n} = B \quad (3)$$



$$\vec{n} = A^\dagger B \quad (4)$$

$$\theta = \cos^{-1} \frac{\vec{a} \cdot \vec{e}}{|\vec{a}| |\vec{e}|} \quad (5)$$

The obtained angle,  $\theta$ , is used to transform the experimental data through rotational transform to match both normal vectors and planes each other. Eq. (6) shows the equation of coordinate transform which transforms experimental data to FE analysis data.  $H$  is rotational matrix depending on  $\theta$  and  $T_c$  is translation vector to move the experimental data to FE model data.  $U_{e,t}$  means transformed experimental displacement field data from  $U_e$ . Fig. 12 shows the final matched both planes and normal vectors through coordinate transform and final transformed displacement field data.

$$U_{e,t} = H(\theta)U_e - T_c \quad (6)$$

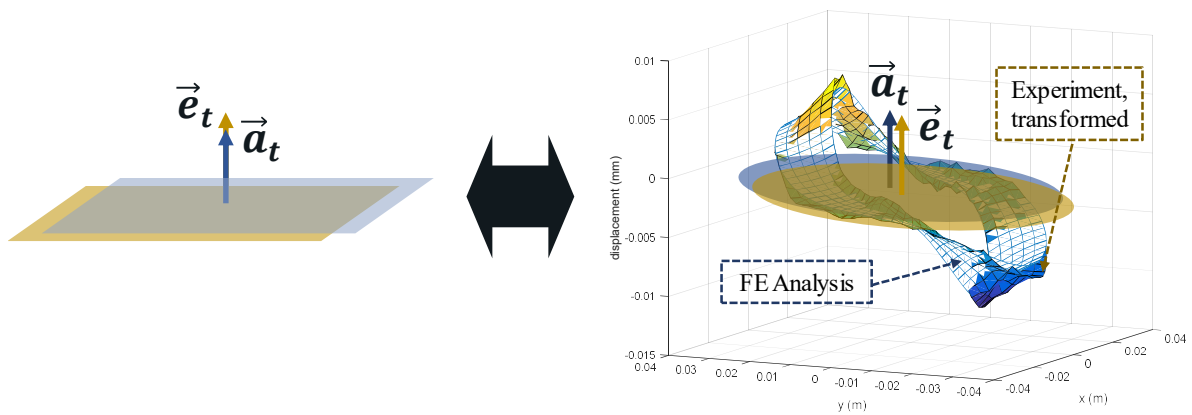


Figure 12. Matched both planes and normal vectors through coordinate transform

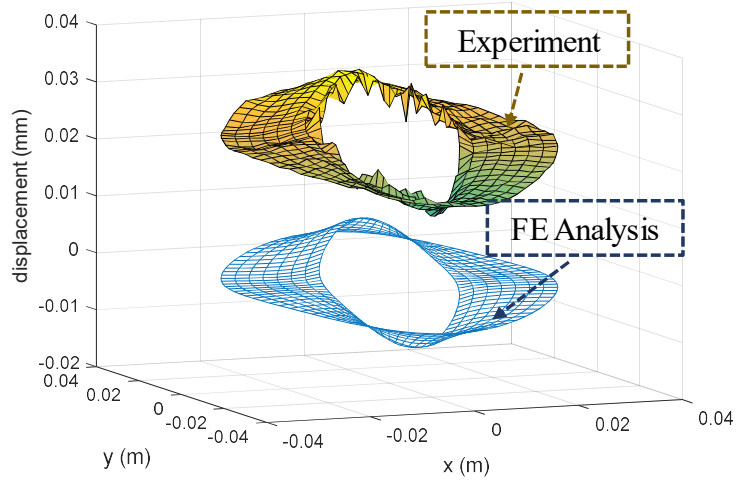
■ **STEP 2: Optimal determination of the static stress**

In the second step, the optimal stress value can be estimated which has the smallest error. In other words, after step 1, the optimal stress can be determined when the difference of two displacement field shapes is minimized as shown in Eq. (7).  $U_f(\sigma)$  varies depending on the stress value,  $\sigma$ , when it is assumed within elastic range.  $U_f(\sigma)$  is then determined when the difference between FE model ( $U_f(\sigma)$ ) and experimental ( $U_{e,t}$ ) displacement field is minimized. Using those values, optimal stress value can be subsequently obtained by using Eq. (8).  $\sigma_{FEM}$  is the stress value in FE analysis when Eq. (7) has the smallest value.

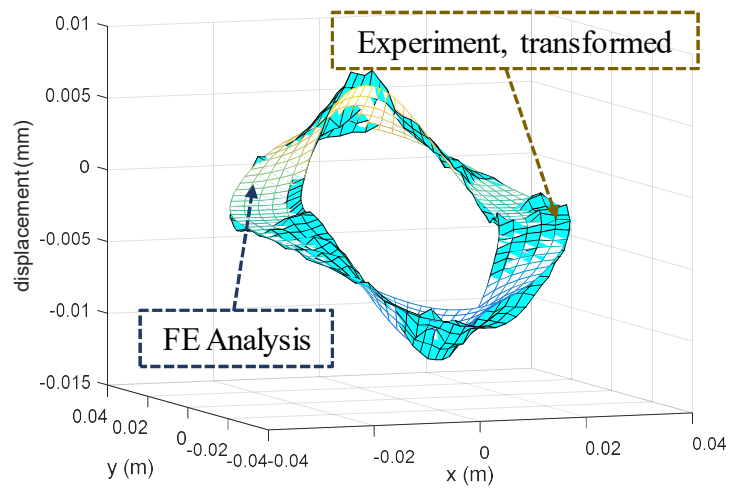
$$\min_{\sigma} \sum (U_f(\sigma) - U_{e,t})^2 \quad (7)$$

$$\sigma = \frac{U_f \cdot U_{e,t}}{U_f \cdot U_f} \sigma_{FEM} \quad (8)$$

Fig. 13(a) shows both displacement field data before data processing and here, reference loading stress of FE analysis data is an applied loading stress during the experiment as shown in Table 2. As shown in Fig. 13(a), two data show some differences and to estimate the static stress, the proposed algorithm is applied. Fig. 13(b) shows the final matched displacement field of both data after conducting static stress estimation algorithm. The optimal stress value can be determined when the difference between them is the smallest.



(a) Original shape of experimental and FE analysis data



(b) Transformed shape of experimental and FE analysis data

**Figure 13. Final transformed displacement field shape of experimental and FE analysis data**

## CHAPTER 4. PARAMETRIC ANALYSIS: Effect of hole diameter and depth

To validate the proposed method, the decision of the hole size, which is used in hole-drilling method, is needed. The purpose of the parametric analysis is to minimize the size of damage which is recovered after experiment in the real field. Parametric analysis is also conducted in FE analysis using ABAQUS. In this study, the important parameters are hole diameter and depth which decide hole size. So, this analysis is performed with changing hole depth and diameter value. The FE modelling condition used in parametric analysis is shown in Table 3 and Fig. 14.

**Table 3. FE modelling condition in parametric analysis**

Concrete specimen size	150mm×150mm×300mm
Elastic modulus	24.9GPa
Hole depth	0 ~ 120mm
Hole diameter	0 ~ 40mm
Loading stress	15MPa
Measured area	Φ80mm ~ Φ140mm

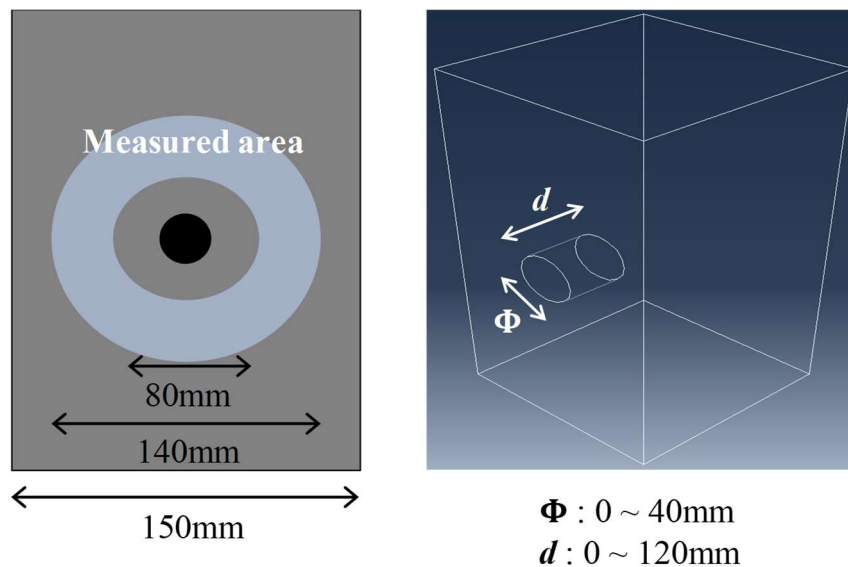
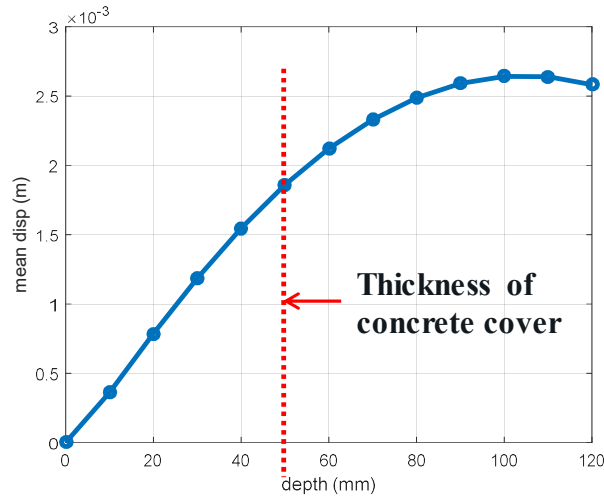
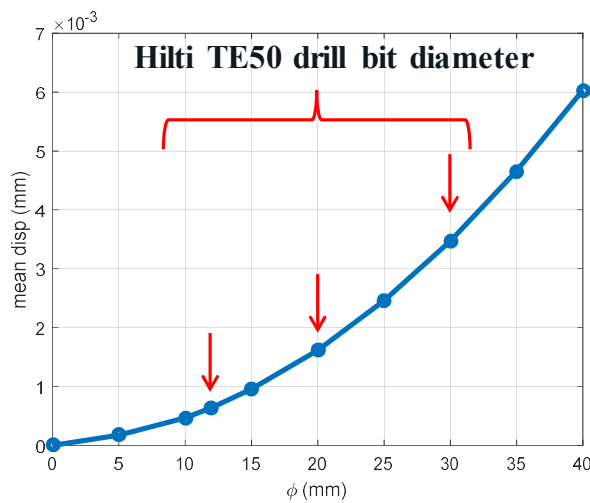


**Figure 14. FE modelling in parametric analysis**



(a) Result with changing depth



(b) Result with changing diameter

**Figure 15. Mean displacement along change of parameters**

Fig. 15(a) is the graph showing the mean displacement value along the depth of the hole when hole diameter is 20mm. The mean released displacement due to hole-drilling is increasing as the hole depth increases. In this case, larger displacement is preferred to measure easily and accurately by DIC. However, as considering that most common concrete cover in reinforced concrete and prestressed concrete is 50mm, the hole depth is determined with 40mm.

Fig. 15(b) is the graph showing the mean displacement value along the diameter of the hole with the fixed hole depth as 40mm. Hole diameter in this parametric study varies from 0 to 40mm. Only three types of drill bits, which are used in the experiment, are sold in the market, and each has a diameter of 12, 20 and 30mm. Because the smaller diameter is needed to minimize the size of damage, the 12mm drill bit is preferred. However, the obtained mean displacement of this case (diameter of 12mm) is too small to be measured with DIC. These small displacements may be hidden in the experimentally generated noise during drilling. Therefore, the hole diameter is decided as 20mm.

## CHAPTER 5. EXPERIMENTAL VALIDATION

In this chapter, the proposed method for estimating the static stress in concrete is validated with laboratory scaled experiments. The incorporation of SRM, DIC, and the developed algorithm for data processing is used to estimate static stress levels of concrete specimens and tested its performance. Experimental setup and test configuration are explained, and final performance results are followed.

### 5.1 Experimental setup

Before stress estimation experiments, preliminary experiments are conducted to decide the ultimate compressive strength and elastic modulus of the concrete specimen. The concrete specimens used in experiments have 24.9GPa of the elastic modulus and 39.3MPa of the ultimate compressive strength which are obtained from the compressive strength test of concrete specimen (see Table 4 and Fig. 16), and 0.17 of Poisson's ratio, which are a general value in concrete. After preliminary experiments, the concrete specimen is under 15MPa loading by universal testing machine (UTM) and it is assumed that this loading strength is within the elastic range because it is under 50% of the compressive strength of the concrete (see Table 4 and Fig. 17). In other words, the concrete specimen is subjected to loads within the elastic range so plastic deformation does not occur during the experiment.



**Figure 16. Compressive strength test on the concrete specimen**

**Table 4. Compressive strength test of concrete specimen**

Specimen	Compressive strength (MPa)	Strain at maximum compressive stress	Experimental elastic modulus, $E_{fc}$ (GPa)
1	38.4	0.0034	18.3
2	39.9	0.0028	31.8
3	40.5	0.0029	24.7
<b>Average</b>	<b>39.3</b>	<b>0.0028</b>	<b>24.9</b>

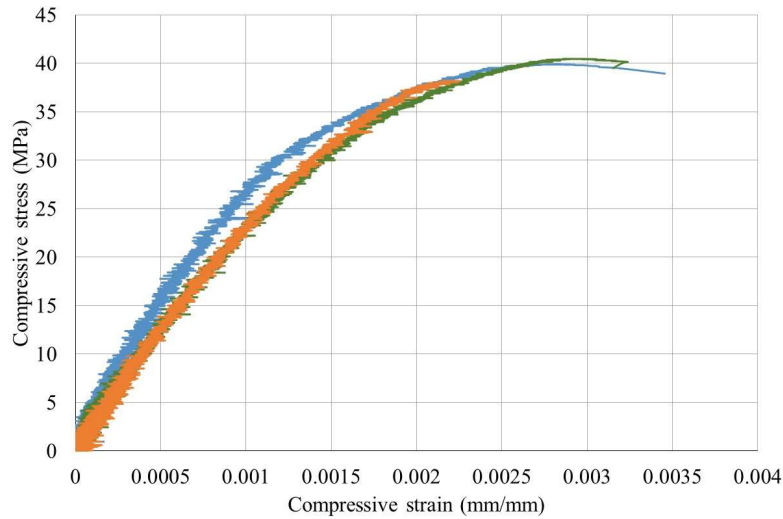
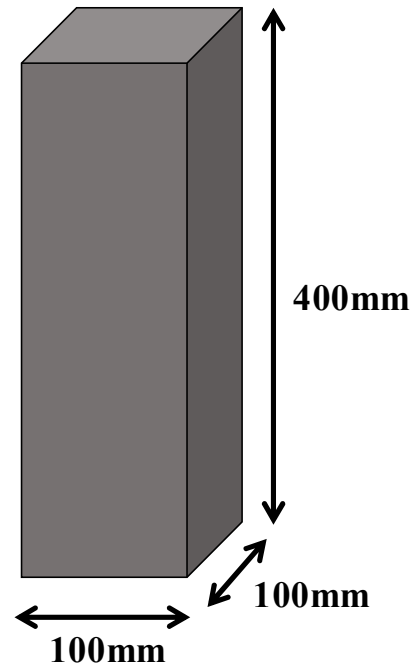


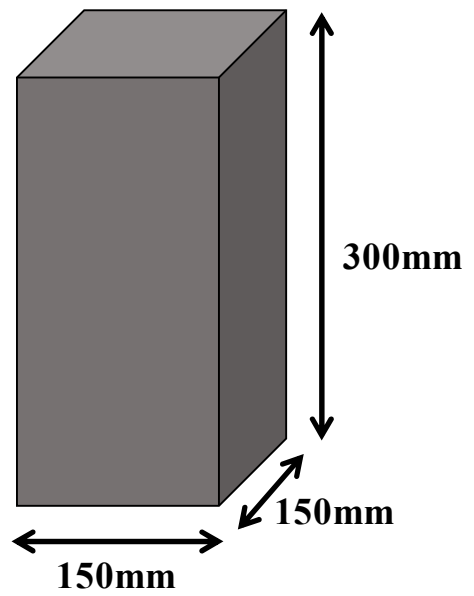
**Figure 17. Stress-strain curve of concrete specimen**

Concrete specimens which is used in experiment are two types; one is 100mm×100mm×400mm, called ‘Type 1’, and the other is 150mm×150mm×300mm, called ‘Type 2’ as illustrated in Fig. 18. Diameter and depth of hole in hole-drilling is 20 mm and 40mm, respectively, which was determined in parametric analysis (in Chapter 4). Random speckled pattern is painted in concrete surface to measure deformation by using DIC (See Figure 18). The speckled pattern is preferred to have more randomness to calculate correlation of each pattern and vision-based deformation measurement is implemented. In this study, DSLR camera is used to take the pictures before and after hole drilling and at this moment, distance from concrete specimen to camera is about 1m. Test configuration is shown in Fig. 19 and experimental condition is represented in Table 5.



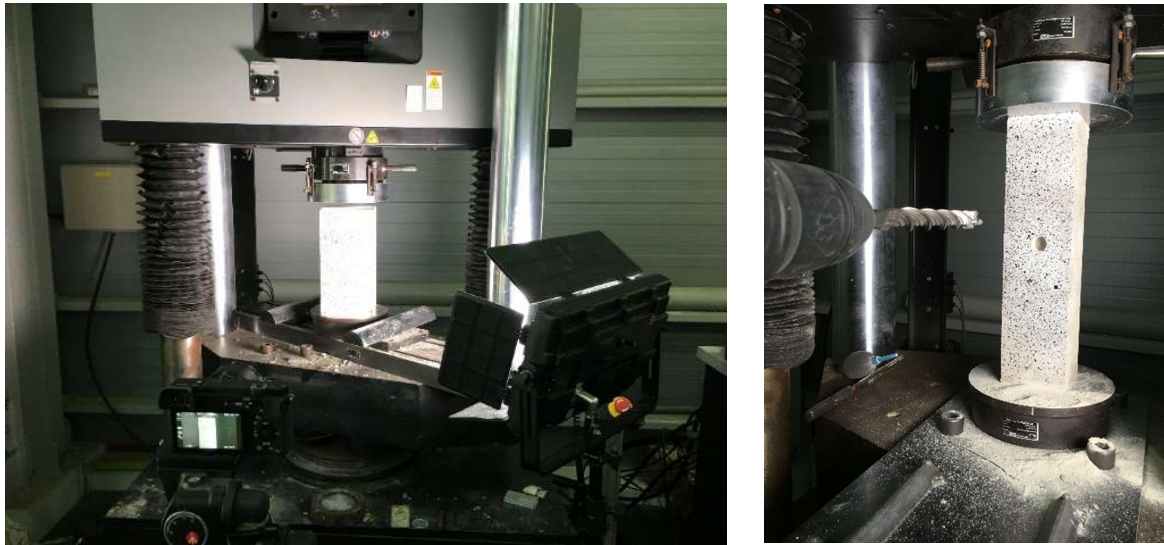


(a) Type 1 concrete specimen



(b) Type 2 concrete specimen

**Figure 18. Concrete specimen dimension**



(a) Test configuration

(b) hold-drilling

**Figure 19. Experimental configuration**

**Table 5. Experimental conditions**

Concrete specimen size	Type 1	100mm×100mm×400mm
	Type 2	150mm×150mm×300mm
Elastic modulus		24.9GPa
Poisson's ratio		0.17
Hole diameter		20mm
Hole depth		40mm
Loading stress		15MPa

## 5.2 Results and analysis

Fig. 20 shows vision-based experimental result of “Type 1” specimen before and after hole-drilling and DIC image processing, respectively. DIC provides the released displacement measurement around the hole after hole-drilling and this displacement data can be used to data processing for estimating the static stress. However, raw displacement data right near the hole have tremendous noise

due to hole-drilling tools (in this case, drill), so some parts should be excluded to minimize the noise effects. Displacement measurement region around the hole is decided empirically through several experiments and it is illustrated with yellow circle in Fig. 20. Fig. 21 shows the experimental results of “Type 1” specimen, specifically “Test 3” among several test results. As comparing the FE modal and experimental measurement field (see Fig. 21(a)) and applying the proposed algorithm, the static stress level of concrete can be estimated. Fig. 21(b) shows the final transformed and matched displacement field shapes of both data and the stress level of this concrete specimen is determined when two data are matched well.

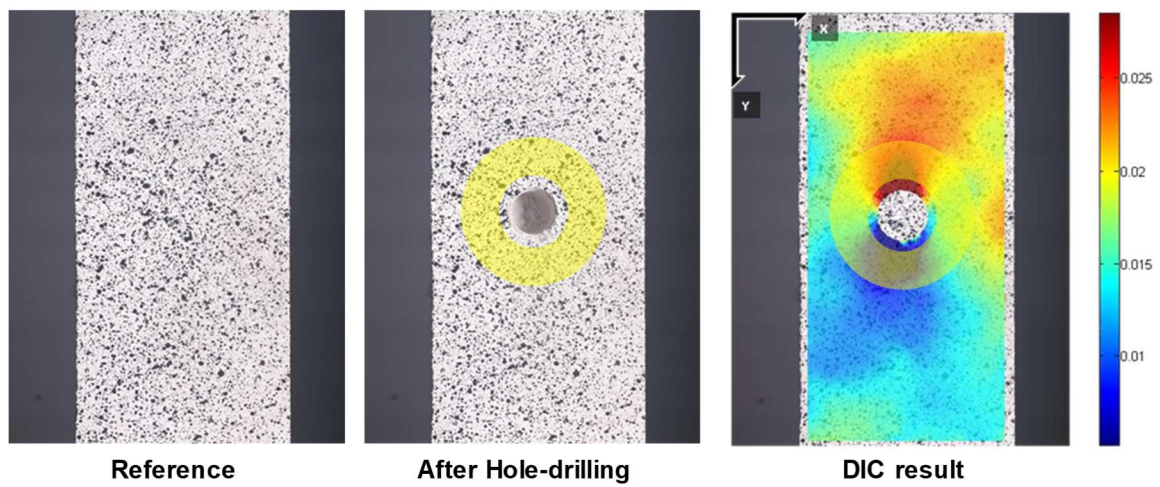
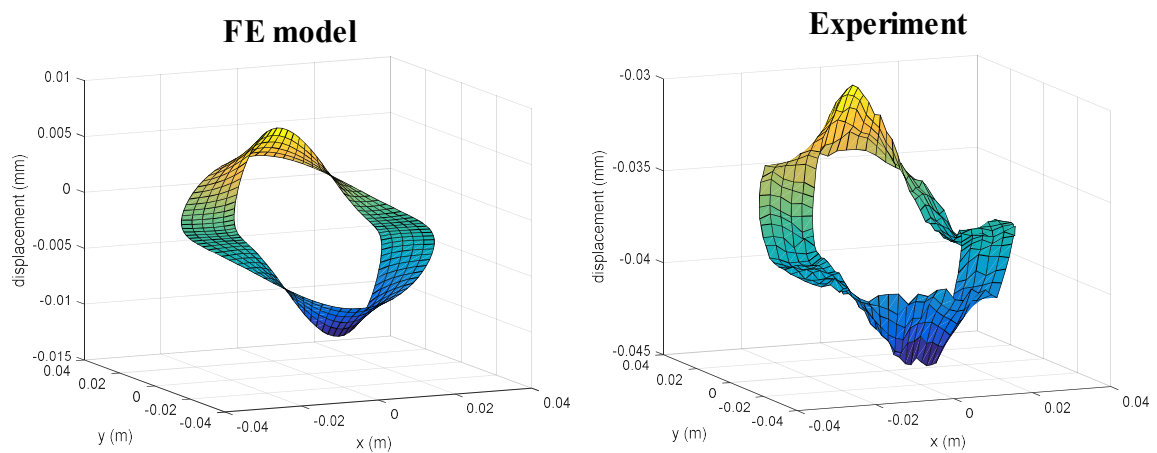
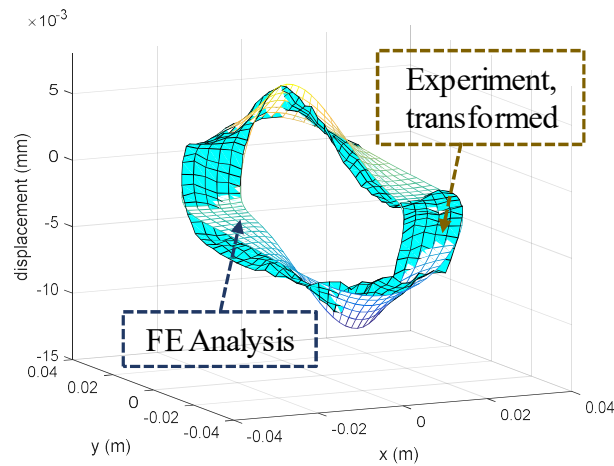


Figure 20. Pictures before and after hole-drilling and DIC results – Type 1\_Test3



(a) Original shape of experimental and FE analysis data



(b) Transformed shape of experimental and FE analysis data

**Figure 21. Experimental results – Type 1\_Test3**

Likewise, Fig. 22 shows the result figures of “Type 2” specimen before and after hole-drilling and DIC processing. Having same process with type 1 specimen, Fig. 23 also shows the final stress estimation results of “Type 2” specimen, specifically “Test 10”. Fig. 23(b) shows the final transformed and matched displacement field shapes of both data. Note that only yellow circle part in Fig. 20 and 22 is considered as a measurement region, which is area from  $\Phi$  35mm to  $\Phi$  45mm from the center of circle.

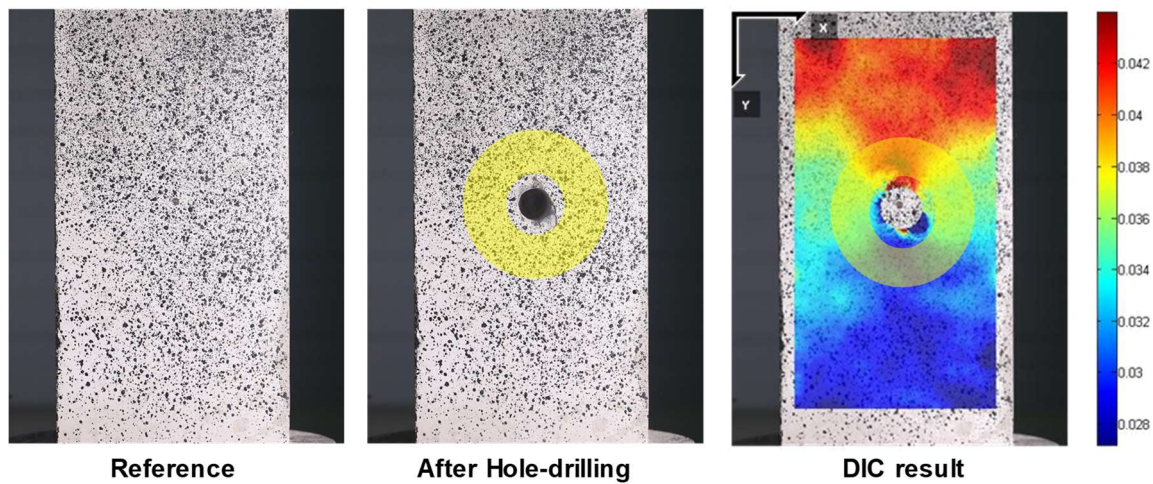
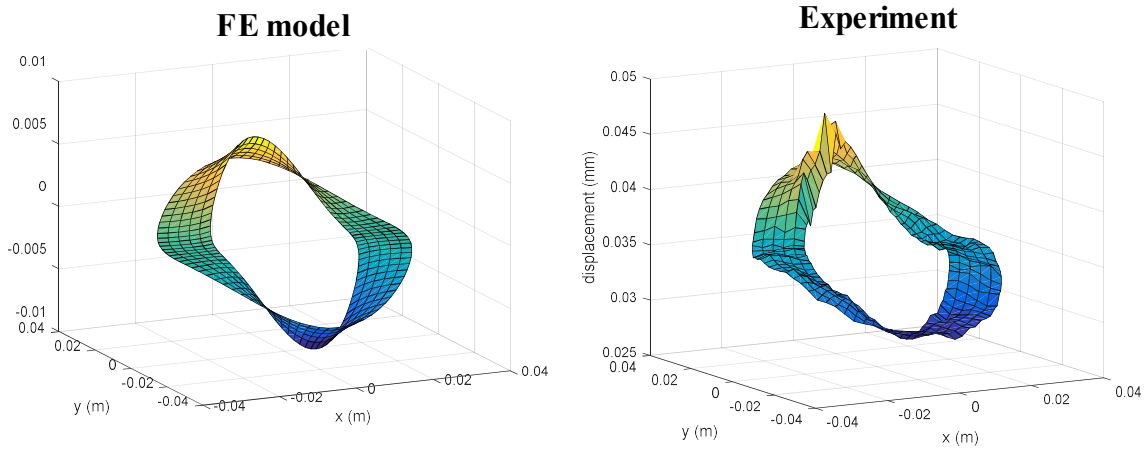
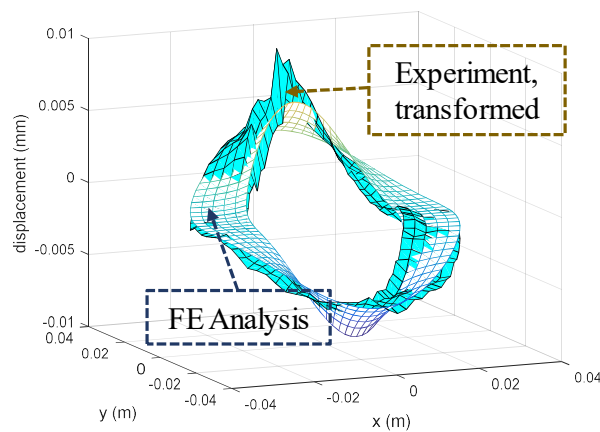


**Figure 22. Pictures before and after hole-drilling and DIC results – Type 2\_Test10**



(a) Original shape of experimental and FE analysis data



(b) Transformed shape of experimental and FE analysis data

**Figure 23. Experimental results – Type 2\_Test10**

Total 13 tests are conducted. ‘Test 1 ~ 9’ are implemented on type 1 specimen and ‘Test 10 ~ 13’ are implemented on type 2 specimen. The experimental results are tabled with estimation stress value and error in Table 6. Average accuracy is found to be 13.6% for all tests, 16% for type 1 specimens and 8% for type 2 specimens. Fig. 24 shows the error bar of each tests. Some results have large error over 20% and it is presumed that some uncertainties of concrete property and experimental condition may be included. Possible things can be that each concrete specimen has different value of elastic modulus

and strength and it is subjected to inhomogeneous loading pressure inducing eccentric load during experiment because of poor-shaped specimen or instrumental problem. In addition, when taking pictures during experiment, camera can be slightly moved due to small vibration during hole-drilling. Change of camera location can make enormous effects to the DIC displacement results since the displacement values covered in this experiment are extremely small as  $10^{-3}$  mm. These mentioned things are still remained to improve in further study. Even though the highest error is over 30%, the proposed method is validated to be able to estimate the static stress state in concrete while reducing the size of damage.

**Table 6. Experimental results**

Test	Specimen type	Reference (MPa)	Estimation (MPa)	Error (%)
1	Type 1	13.8	14	1.45
2	Type 1	13.8	15.1	9.42
3	Type 1	13.6	12.4	8.82
4	Type 1	13.8	11	20.3
5	Type 1	14.1	13	7.8
6	Type 1	14.2	16	12.68
7	Type 1	13.8	17.1	23.91
8	Type 1	13.2	16.7	26.52
9	Type 1	14	9.3	33.57
10	Type 2	13.5	12.7	5.93
11	Type 2	13.95	13.7	1.79
12	Type 2	14.1	12	14.89
13	Type 2	14	12.6	10
<b>Average</b>				<b>13.6</b>

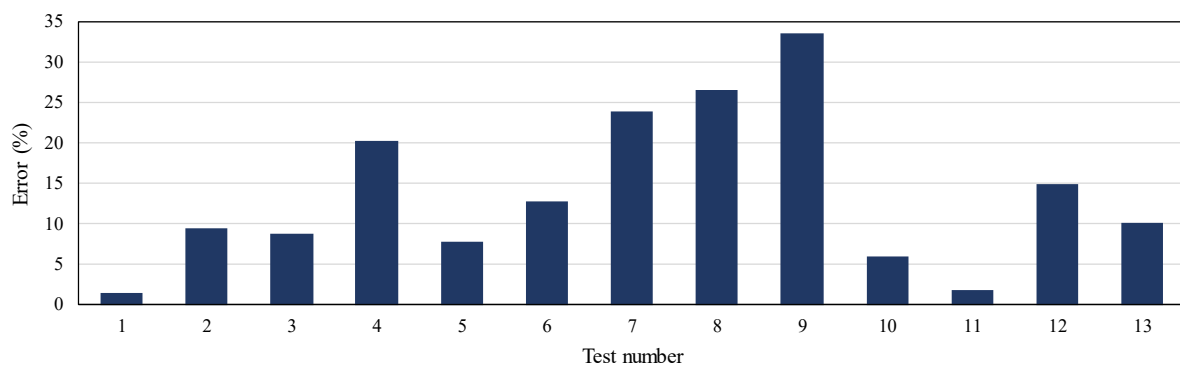


**Figure 24. Experimental results**

## CHAPTER 6. CONCLUSION

As increasing issue about structural safety, demand to identify and monitor the current state of structure is also increasing. Most structures have been built of concrete, so technique to diagnose the safety of concrete structures becomes important. One of such techniques is to evaluate the current stress state in concrete. Current stress level in concrete is important factor to check the safety level and load distribution in the structures in service. Objective of this study is to develop static stress estimation technique which can be applied to real concrete structures. This study proposed the semi-destructive static stress evaluation technique with incorporating the stress relaxation method (SRM) and computer vision-based digital image correlation (DIC).

The existed static stress in concrete could be released by SRM, in this study, hole-drilling method was used. Released deformation by stress relaxation was captured by DIC and static stress could be estimated based on the relaxed displacement. Note that the full-field released displacement around a hole can be measured through DIC. FE model of concrete specimen was modelled as a reference using commercial numerical modelling software and it was used in developed static stress estimation algorithm with experimental data. Main idea of the proposed method is to find the optimal stress value which makes minimum difference between FE analysis data and experimental data. Parametric analysis was conducted to decide the optimal hole size to minimize damage in concrete. The proposed method including the results of parametric analysis was validated with several laboratory-scaled experiments on concrete specimens loaded by the universal testing machine. Total 13 tests were conducted; Test 1~9 were conducted on type 1 specimen and Test 10~13 were conducted on type 2 specimen. Even though some results showed large error, overall static stress estimation results for concrete were estimated with 13.6% average error.

This study has some limitations to apply immediately to real structures. Because of some large errors in conducted experiments, it is needed to improve accuracy for applying to real structures. This study considers only uniaxial loading condition whereas the real structures can be loaded by uniaxial, biaxial or multiaxial loading stress. It is necessary to strengthen the performance of the algorithm for successfully estimating the static stress of concrete even under the multiaxial load conditions. The other improvement thing is a decision of measurement region which was decided empirically. By obtaining more experimental results, the optimal measurement region can be determined that makes minimum estimating error. Meanwhile, some efforts considering uncertainties of concrete and taking images at flexible location should be also followed in further study to apply to real structures with high accuracy.

With mentioned further improvements, this technique will be expected to investigate a safety assessment of the concrete structures.

To summarize the conclusions,

- In this study, a DIC-based technique was developed for evaluation of static stress on concrete incorporating the stress relaxation method.
- Static stress estimation algorithm was developed and verified through experiments on lab-scaled specimens.
- Accuracy of experiments was found to be about 14%.
- With further improvements, this technique is expected to be useful for safety assessment of aged concrete structures.



## REFERENCES

1. Hernandez, H.D., & Gamble, W.L. (1975). Time-dependent prestress losses in pre-tensioned concrete construction. University of Illinois Engineering Experiment Station, College of Engineering, University of Illinois at Urbana-Champaign, Champaign, IL.
2. Hognestad, E., Hanson, N. W., & McHenry, D. (1955). Concrete stress distribution in ultimate strength design. *Journal of the American Concrete Institute*, 52(57), 455–479.
3. Vecchio, F. J., Lai, D., Shim, W., & Ng, J. (2001). Disturbed stress field model for reinforced concrete: validation. *Journal of Structural Engineering*, 127(4), 350–358.
4. Park, D. S., & Kim, W. (2006). An Experimental Method for the Evaluation of Dead Load Stress in Existing Concrete Bridges. *Journal of The Korean Society of Civil Engineers*, 26(4A), 701-706.
5. Popovics, S. (1970). A review of stress-strain relationships for concrete. *ACI Journal*, 67(3), 243-248.
6. Popovics, S. (1973). A numerical approach to the complete stress-strain curve of concrete. *Cement and Concrete Research*, 3(5), 583–599.
7. Carreira, D. J., & Chu, K. H. (1985). Stress-strain relationship for plain concrete in compression. *ACI Journal*, 82(6), 797-804.
8. Harajli, M. H., Hantouche, E., & Soudki, K. (2006). Stress-strain model for fiber-reinforced polymer jacketed concrete columns. *ACI Structural Journal*, 103(5), 672–682.
9. Saetta, A., Scotta, R., & Vitaliani, R. (1995). Stress analysis of concrete structures subjected to variable thermal loads. *Journal of Structural Engineering*, 121(3), 446-457.
10. Fedele, R., & Maier, G. (2007). Flat-jack tests and inverse analysis for the identification of stress states and elastic properties in concrete dams. *Meccanica*, 42(4), 387–402.
11. Fedele, R., Maier, G., & Miller, B. (2005). Identification of elastic stiffness and local stresses in concrete dams by in situ tests and neural networks. *Structure and Infrastructure Engineering*, 1(3), 165-180.
12. Owens, A. (1993). In-situ stress determination used in structural assessment of concrete structures. *Strain*, 29(4), 115-124.

13. Pessiki, S., & Turker, H. T. (2003). Theoretical Development of the Core-Drilling Method for Non destructive Evaluation of Stresses in Concrete Structures.
14. McGinnis, M. J., Pessiki, S., & Turker, H. (2005). Application of three-dimensional digital image correlation to the core-drilling method. *Experimental Mechanics*, 45(4), 359–367.
15. McGinnis, M., Pessiki, S., & Li, Z. (2007). Review of the core-drilling method for evaluating concrete stresses. *Proc. of International Conference on Health Monitoring of Structure, Materials and Environment*, Vols 1 and 2.
16. Trautner, C., McGinnis, M. J., & Pessiki, S. (2010). Analytical and numerical development of the incremental core-drilling method of non-destructive determination of in-situ stresses in concrete structures. *The Journal of Strain Analysis for Engineering Design*, 45(8), 647–658.
17. Parivallal, S., Ravisankar, K., Nagamani, K., & Kesavan, K. (2011). CORE-DRILLING TECHNIQUE FOR IN-SITU STRESS EVALUATION IN CONCRETE STRUCTURES. *Experimental Techniques*, 35(4), 29-3.
18. Trautner, C., McGinnis, M., & Pessiki, S. (2011). Application of the Incremental Core-Drilling Method to Determine In-Situ Stresses in Concrete. *ACI Materials Journal*, 108(3).
19. McGinnis, M. J., & Pessiki, S. (2015). Experimental Study of the Core-Drilling Method for Evaluating In Situ Stresses in Concrete Structures. *Journal of Materials in Civil Engineering*, 28(2), 04015099.
20. Ruan, X., & Zhang, Y. (2015). In-situ stress identification of bridge concrete components using core-drilling method. *Structure and Infrastructure Engineering*, 11(2), 210–222.
21. Mathar, J. (1934). Determination of initial stresses by measuring the deformation around drilled holes. *Transactions ASME*, 56(4), 249–254.
22. Šarga, P., & Menda, F. (2013). Comparison of ring-core method and hole-drilling method used for determining residual stresses. *American Journal of Mechanical Engineering*, 1(7), 335-338.
23. Schajer, G. S. (2010). Advances in hole-drilling residual stress measurements. *Experimental mechanics*, 50(2), 159-168.
24. ASTM. (2008). Determining Residual Stresses by the Hole-Drilling Strain-Gage Method. *Standard Test Method E837-13a*, i, 1–16.
25. ASTM. (2008). Standard test method for determining residual stresses by the hole-drilling strain-

- gage method. Standard Test Method E837-13a. America Society for Testing and Materials.
26. ASTM. (2013). Standard Test Method for Determining Residual Stresses by the Hole-Drilling Strain-Gauge Method. Standard Test Method E837-13a, 3, 1–16. <https://doi.org/10.1520/E0837-13A.2>
  27. Niku-Lari, A., Lu, J., & Flavenot, J. F. (1985). Measurement of residual-stress distribution by the incremental hole-drilling method. *Journal of Mechanical Working Technology*, 11(2), 167–188.
  28. Sicot, O., Gong, X. L., Cherouat, a., & Lu, J. (2003). Determination of Residual Stress in Composite Laminates Using the Incremental Hole-drilling Method. *Journal of Composite Materials*, 37(9), 831–844.
  29. Santana, Y. Y., La Barbera-Sosa, J. G., Staia, M. H., Lesage, J., Puchi-Cabrera, E. S., Chicot, D., & Bemporad, E. (2006). Measurement of residual stress in thermal spray coatings by the incremental hole drilling method. *Surface and Coatings Technology*, 201(5), 2092–2098.
  30. Nelson, D. V., Makino, A., & Schmidt, T. (2006). Residual stress determination using hole drilling and 3D image correlation. *Experimental Mechanics*, 46(1), 31–38.
  31. Group, V. P. (2010). Measurement of Residual Stresses by the Hole-Drilling\* Strain Gage Method. Tech Note TN-503, 11053, 19–33.
  32. Lyons, J. S., Liu, J., & Sutton, M. a. (1996). High-temperature deformation measurements using digital-image correlation. *Experimental Mechanics*, 36(1), 64–70.
  33. Chen, J., Xia, G., Zhou, K., Xia, G., & Qin, Y. (2005). Two-step digital image correlation for micro-region measurement. In *Optics and Lasers in Engineering*, 43, 836–846.
  34. Yoneyama, S., Kitagawa, A., Iwata, S., Tani, K., & Kikuta, H. (2007). Bridge deflection measurement using digital image correlation. *Experimental Techniques*, 31(1), 34–40.
  35. Withers, P. J. (2008). Strain measurement by digital image correlation. *Strain*, 44(6), 421–422.
  36. Pan, B., Qian, K., Xie, H., & Asundi, A. (2009). Two-dimensional digital image correlation for in-plane displacement and strain measurement: a review. *Measurement Science and Technology*, 20(6), 62001.
  37. Kozicki, J., & Tejchman, J. (2013). Application of DIC technique to concrete—study on objectivity of measured surface displacements. *Experimental Mechanics*, 53(9), 1545-1559.
  38. Gencturk, B., Hossain, K., Kapadia, A., Labib, E., & Mo, Y.-L. (2014). Use of digital image

- correlation technique in full-scale testing of prestressed concrete structures. *Measurement*, 47, 505–515.
39. De Wilder, K., Lava, P., Debruyne, D., Wang, Y., De Roeck, G., & Vandewalle, L. (2015). Experimental investigation on the shear capacity of prestressed concrete beams using digital image correlation. *Engineering Structures*, 82, 82–92.
40. Ncorr v.1.2. (2015). Retrieved November 26, 2017, <http://www.ncorr.com/index.php>
41. Harilal, R. & Ramji, M. (2014). Adaptation of open source 2D DIC software Ncorr for solid mechanics applications. In *Proceedings of the 9th international symposium on advanced science and technology in experimental mechanics (ISEM '14)*. New Delhi.
42. Blaber, J., Adair, B., & Antoniou, A. (2015). Ncorr: Open-Source 2D Digital Image Correlation Matlab Software. *Experimental Mechanics*, 55(6), 1105–1122.